HHS Public Access

Author manuscript

Prostaglandins Other Lipid Mediat. Author manuscript; available in PMC 2024 December 01.

Published in final edited form as:

Prostaglandins Other Lipid Mediat. 2023 December ; 169: 106769. doi:10.1016/j.prostaglandins.2023.106769.

A Novel *HSPB1*^{S139F} Mouse Model of Charcot-Marie-Tooth Disease

Keila S. Espinoza[1,*], **Kyra N. Hermanson**[1,*], **Cameron A. Beard**[2], **Nicholas U. Schwartz**[3], **Justin M. Snider**[2,4], **Benjamin E. Low**[5,6], **Michael V. Wiles**[5], **Yusuf A. Hannun**[7,8], **Lina M. Obeid**[7,8], **Ashley J. Snider**[2,4]

[1]Department of Physiology, University of Arizona, Tucson, AZ 85721, USA

[2]School of Nutritional Sciences and Wellness, University of Arizona, Tucson, AZ 85721, USA

[3]Department of Neurology, Stanford University Medical Center, Stanford, CA 94304, USA

[4]University of Arizona Cancer Center, University of Arizona, Tucson, AZ 85721, USA

[5]Technology Evaluation and Development, The Jackson Laboratory, Bar Harbor, Maine, USA

[6]Genetic Resource Science, The Jackson Laboratory, Bar Harbor, Maine, USA

[7]Department of Medicine and Stony Brook Cancer Center, Stony Brook, NY 11794, USA

[8]Northport Veterans Affairs Medical Center, Northport, NY 11768, USA

Abstract

Charcot-Marie-Tooth Disease (CMT) is a commonly inherited peripheral polyneuropathy. Clinical manifestations for this disease include symmetrical distal polyneuropathy, altered deep tendon reflexes, distal sensory loss, foot deformities, and gait abnormalities. Genetic mutations in heat shock proteins have been linked to CMT2. Specifically, mutations in the heat shock protein B1 (*HSPB1*) gene encoding for heat shock protein 27 (Hsp27) have been linked to CMT2F and distal hereditary motor and sensory neuropathy type 2B (dHMSN2B) subtype. The goal of the study was to examine the role of an endogenous mutation in HSPB1 *in vivo* and to define the effects of this mutation on motor function and pathology in a novel animal model. As sphingolipids have been implicated in hereditary and sensory neuropathies, we examined sphingolipid metabolism in central and peripheral nervous tissues in 3-month-old Hsp^{S139F} mice. Though sphingolipid

Corresponding Author: Ashley J. Snider, Ph.D., ashleysnider@arizona.edu, 1230 N Cherry Ave, BSRL 372, Tucson, AZ 85721, Phone: +1-520-621-8093.

*these authors contributed equally to this work

Author contributions

KSE and KNH wrote the manuscript, performed conceptual and experimental design, as well as generation of data and analyses for experiments. JMS assisted with data analysis and manuscript editing. CAB performed locomotor and coordination experiments. NUS assisted with conceptualization and design for the endogenous point mutation. BEL and MVW generated the CRISPR mice. YAH and LMO contributed to experimental design, data analysis and manuscript editing. AJS conceived the original hypothesis, provided the necessary funding for materials and methods, and supervised the project.

Disclosures

All authors declare that they have no conflicts of interest.

levels were not altered in sciatic nerves from Hsp^{S139F} mice, ceramides and deoxyceramides, as well as sphingomyelins (SMs) were elevated in brain tissues from Hsp^{S139F} mice. Histology was utilized to further characterize Hsp^{S139F} mice. Hsp^{S139F} mice exhibited no alterations to the expression and phosphorylation of neurofilaments, or in the expression of acetylated α-tubulin in the brain or sciatic nerve. Interestingly, Hsp^{S139F} mice demonstrated cerebellar demyelination. Locomotor function, grip strength and gait were examined to define the role of Hsp^{S139F} in the clinical phenotypes associated with CMT2F. Gait analysis revealed no differences between Hsp^{WT} and Hsp^{S139F} mice. However, both coordination and grip strength were decreased in 3-month-old Hsp^{S139F} mice. Together these data suggest that the endogenous S139F mutation in HSPB1 may serve as a mouse model for hereditary and sensory neuropathies such as CMT2F.

Keywords

Charcot-Marie-Tooth 2F (CMT2F); ceramide synthase (CerS); hereditary sensory and autonomic neuropathy type 1 (HSAN1); phospho-neurofilament; acetylated α-tubulin

INTRODUCTION

Charcot-Marie-Tooth Disease (CMT) is an inherited peripheral polyneuropathy estimated to affect every 1 in 2500 people (1). Clinical phenotypes for this disease comprise symmetrical distal polyneuropathy (2, 3), decreased or absent deep tendon reflexes, distal sensory loss, foot deformities such as *pes cavus* (hammer toes), and gait abnormalities (4-6). CMT is analogously named hereditary motor and sensory neuropathy (7), corresponding to the initial description of the disease. More than 70 genes have been implicated in CMT (8), with the majority of these mutations falling into one of two major subtypes: CMT1 and CMT2. CMT1 is most prevalent, encompassing 80% of cases, and has been classified by the demyelination of neurons; this results in reduced motor nerve conduction velocity of the motor neuron (8). CMT2 does not affect nerve conduction velocity, but has been defined by axonal damage, resulting in reduced compound muscle action potential (8).

Genetic mutations in heat shock proteins have been linked to CMT2. Specifically, mutations in the heat-shock protein B1 (*HSPB1*) gene, which encodes for heat shock protein 27 (Hsp27), have been linked to the CMT2F subtype (9). Hsp27 is part of the family of small Hsps which are chaperone proteins important for cellular protein homeostasis (10). Hsp27 has also been shown to provide neuroprotective effects as well as protection against oxidative stress, aging, and apoptosis (10-12). To better understand the underlying mechanisms that cause the pathophysiology seen in CMT2F, many cell lines and mouse models have been generated; however, the conclusions from these studies have not been definitive (13).

Sphingolipids, which have been implicated in hereditary and sensory neuropathies, are generated *de novo* by the condensation of serine and palmitoyl-CoA by serine palmitoyl transferase (SPT) which following several enzymatic steps leads to the generation of ceramide. Mutations in SPT are implicated in hereditary sensory and autonomic neuropathy type 1 (HSAN1) via the accumulation of deoxysphingolipids (14), resulting in similar phenotypes to CMT2F. Ceramide serves as the central lipid in sphingolipid metabolism

and can regulate cell growth, senescence, proliferation, differentiation, and apoptosis (15). The generation of ceramide is catalyzed by one of six ceramide synthases (CerS) each with fatty acid specificity, resulting in the generation of specific species of ceramide (16). CerS1, which catalyzes the formation of C18 and C18:1 ceramide(s) (17, 18), is highly expressed in the nervous system, skeletal muscle, and testes (19, 20). Deficiency in CerS1 result in decreased ceramide levels, degeneration of cerebellar Purkinje cells and lipofuscin accumulation (21). CerS2, which incorporates very-long chain (VLC; C22-C24) fatty acids into ceramides, has been suggested to regulate myelination (22). In mouse hippocampal neuronal (HT-22) cells, mutant Hsp27 S135F has been shown to decrease localization of CerS1 to the mitochondria (23). These studies implicate the potential for sphingolipids and their generating enzymes in other HSANs such as CMT.

Despite the prevalence of CMT disease there are limited treatments and early diagnostics available. This current study sought to characterize a novel mouse model for CMT2F. These mice contain a S139F mutation in mouse Hsp25, which corresponds to the S135F point mutation in human Hsp27; a common mutation in CMT2F. The data presented here suggest HSP^{S139F} mice may be an *in vivo* model to study CMT2F or dHMSN2B.

METHODS AND MATERIALS

Generation of HSP^{S139F} mice

To generate the HSP^{S139F} mice, female C57BL/6J mice (JAX stock# 000664) were superovulated and mated. Zygotes were collected and microinjected with ~2–5 pl of a mixture as previously described (57). The microinjection mixture contained: Cas9 mRNA (Trilink, 100 ng/μl), Cas9 protein (PNABio, 50 ng/μl), a single-guide RNA (sgRNA#2165, 50 ng/μl) and an 83nt oligonucleotide donor (Integrated DNA Technologies, oligo#2169, 3 ng/μl). Designed as a truncated guide to reduce off-target potential (60), we used the online software tool “Breaking-Cas” (https://bioinfogp.cnb.csic.es/tools/breakingcas; 58), to identify sgRNA#2165, which targets the sequence: 5’-GAACATGGCTACATCTCT. The template for homology-directed repair (oligo#2169) was designed as an asymmetric oligonucleotide donor (59): 5’-GCCCTCCATGCAAGGAATCAGAACTCACGTGTATTTCCGGGTGAAGCACCGA(A)AGATGTAGCCATGTTCGTCCTGCCTTTCTT. This mixture was designed to generate a cytosine to thymine point mutation (TCT to TTT) in the codon for serine at position 139 in the murine *HSPB1* gene. Of 18 offspring, at least 6 founders appeared to have the intended mutation in *HSPB1* as detected by PCR and sequencing. Founders were backcrossed to wild-type (WT) C57BL/6J mice, and N1 heterozygotes ($HSP^{S139F/+}$) with only the point mutation at S139F were selected to establish the HSP^{S139F} C57BL/6J strain, designated C57BL/6J-*Hspb1*^{em1Mvw}/Mvw (stock # 030923; The Jackson Laboratory) and abbreviated here to HSP^{S139F} mice. Note, with 100% homology, the sgRNA#2165 was predicted to also cut in a pseudogene on Chromosome 13 (Hsp25-ps1), and indeed all six of the founder animals contained edits at this site when screened. However, stock# 030923 was established using only mice that carried the HSP^{S139F} allele on Chromosome 5 and the WT form of Hsp25-ps1 on Chromosome 13 (i.e., after segregation of the unintended targeting event).

Genotypes of the offspring were confirmed via genetic sequencing and male and female mice were used for experiments. All animal experiments were approved by the University of Arizona Institutional Animal Care and Use Committee and followed US National Institutes of Health “Using Animals in Intramural Research” guidelines for animal use and the guidelines of the American Veterinary Medical Association.

Rotarod testing

Coordination of mice was tested using Rotarod Rotamex 5 (Columbus Instruments, Columbus, Ohio, USA). Mice were placed individually in one of four lanes of the instrument and recorded simultaneously. Rod speed started at 4 RPM and the rod speed increased 0.5 RPM every 5s until the mouse could no longer maintain the speed. Testing was conducted three separate times with twelve minutes rest between and averaged for analyses.

Grip strength testing

Muscular grip strength of mice was measured using a Grip Strength Meter (Columbus Instruments, Columbus, Ohio, USA). A square metal grid was attached to the meter and used for both forepaw and all paw clasping. Mice were handled by the base of their tails and allowed to grip the metal grid. The mice were then gently and consistently pulled, and grip strength was recorded in grams force. A total of five recordings were taken with five minutes rest between and the average used for analyses.

Mass spectrometry for quantitation of sphingolipids

Sphingolipids were measured as done previously (24-26). Briefly, tissues were homogenized with glass beads using MP Biomedicals FastPrep-24 in 1 mL cell extraction solvent (2:3, 70% isopropanol/ethyl acetate). Sample extract was transferred to glass tubes containing appropriate internal standards and dried down under nitrogen, and then resuspended in mobile phase (1 μM ammonium formate, 2% formic acid in MEOH). Analyses were conducted at Stony Brook University on an HESI probe enabled TSQ Quantum Ultra triple quad mass spectrometer tandem Accela 1250 HPLC system. Further analysis of collected data was performed by the University of Arizona Cancer Center Analytical Chemistry Shared Resource Core. Data were normalized to total lipid phosphate (Pi) (27, 28) and represented as pmol/nmol of lipid Pi.

Immunofluorescence

Mice were anesthetized under isoflurane anesthesia and perfused with 10% formalin (Masterflex Pump Cole-Parmer® Instruments, Vernon Hills, IL, USA). Brain and sciatic nerve tissues were harvested, kept in 10% formalin for 24 hours and then were transferred into 70% ETOH. Samples were processed, embedded, and sectioned by the University of Arizona Cancer Center (UACC) Tissue Acquisition & Cellular/Molecular Analysis Shared Resource (TACMASR). Tissue slides were deparaffinized at 60°C for 1 hour in a STRATAGENE Hybridizer 600 (Decisive Diagnostics, Jackson, WY, USA) and rehydrated stepwise in 100% Xylene, 100%, 95%, and 70% ETOH, followed by ddH20 and 1x phosphate buffered saline PBS. Antigen retrieval was achieved in a decloaking chamber (BioCare Medical, Pacheo, CA, USA) in 1x citrate buffer heated to 95°C for 45 min.

Tissues were blocked in 10% goat serum + 5% BSA in 1x tris phosphate buffered saline with 0.1% Tween 20 (TBS-T). Acetylated anti-α tubulin (ab179484) and anti-neurofilament light antibodies (ab223343) (Abcam, Fremont, CA, USA) were used at dilutions 1:800, and phospho-neurofilament heavy (sc-32730, Santa Cruz Biotechnology, Dallas, TX, USA) at 1:100. Texas Red goat anti rabbit secondary antibody (ab6719, Abcam, Fremont, CA, USA) was used at dilutions 1:1000. No antibody and secondary only antibody controls were used. For myelin staining, slides were incubated at 56°C overnight in Luxol Fast Blue (S3382-25G, MilliporeSigma, KGaA, Dremstadt, Germany). Slides were rinsed in 95% ethanol, differentiated in 0.05% lithiam carbonate for 30 seconds, 70% ethanol for 30 seconds, and rinsed in distilled water. Tissues were counterstained in 0.1% Cresyl Violet solution (ab246816, Abcam, Fremont, CA, USA) for 30 seconds, then dehydrated in 95%-100% ethanol and xylenes prior to mounting. All slides were mounted using Vecta Shield mounting medium (Vector Laboratories, Burlingame, CA, USA).

Statistical Analysis

Analysis Software GraphPad Prism 9 (Boston, MA, USA) was used. Data were analyzed using 2-Way ANOVA with Tukey Multiple Testing Corrections.

RESULTS

Generation of the novel HSP^{S139F} mouse

Previous studies investigating CMT have utilized transgenic mouse models harboring mutations in human proteins or *HSPB1* knockout (KO) mice (29); however, these mouse models may not accurately reflect the effects of mutations in the endogenous Hsp25 protein and don't account for endogenous Hsp25 activity. Therefore, to generate a novel mouse model containing a mutation in the endogenous mouse *HSPB1* gene, CRISPR-Cas9 technology was used, creating a potential new model for the study of CMT2F. In collaboration with Jackson Laboratory, a novel genetically modified mouse model containing a point mutation in *HSPB1* was generated, creating a S139F mutation in the mouse Hsp25 that corresponds to the S135F mutation found in the human Hsp27 protein (Table 1). Genetic sequencing confirmed a homozygous cytosine to thymine point mutation resulting in a shift from serine to phenylalanine at this position. These mice harboring the S139F mutation in the endogenous Hsp25 protein were then characterized as a potential novel mouse model for CMT2F.

CRISPR-Cas9 technology was used to generate a novel mouse model containing a mutation in the endogenous mouse *HSPB1* gene. A homozygous cytosine to thymine point mutation was introduced at S139F in the mouse *HSPB1* corresponding to the S135F mutation in humans.

HSP^{S139F} mice accumulate ceramides, sphingomyelins, and deoxyceramides

Studies by Schwartz et. al. demonstrated altered ceramide metabolism in sciatic nerves, but not brain tissues from *HSPB1* KO mice (23). In addition to decreases in total ceramides, VLC ceramides (C20, C22, C24 and C26) were decreased in sciatic nerves from *HSPB1* KO mice (23). Alterations in ceramide and deoxyceramide levels have been

implicated in HSAN, neurodegeneration and Purkinje cell death (22, 30, 31). Therefore, mass spectrometry was utilized to measure lipid species in central and peripheral nervous tissues. Sciatic nerves from HSP^{S139F} mice exhibited no alterations in ceramide levels in comparison to HSP^{WT} mice (Table S1); however, C14, C18 and C18:1 SM levels were significantly higher in HSP^{S139F} mice (Table S2). Next, sphingolipid levels in brain tissues were measured from HSP^{WT} and HSP^{S139F} mice. Total ceramide levels as well as sphingosine-1-phosphate (S1P) were not different between genotypes (Figure 1A & B). Sphingosine, C16 ceramide, and several species of VLC ceramides (C22, C24:1, C24, and C26) were elevated in the brains of HSP^{S139F} mice as compared to HSP^{WT} at 3 months of age (Figure 1C-H). Deoxysphinganine and deoxydihydroceramides were not altered (data not shown); however, deoxyceramides were significantly elevated in brain tissues from HSP^{S139F} mice (Figure 1I). Total SMs were also elevated in the brain tissues form HSP^{S139F} mice (Figure 2A). Specific long-chain SM were significantly higher in HSP^{S139F} mice, including C18 and C18:1, but not C16 (Figure 2B-D). Similar to ceramide levels in the brain, several species of VLC SMs (C22, C24 and C26:1) were significantly increased in HSP^{S139F} mice (Figure 2E-H). These data demonstrate that while sphingolipid metabolism is not significantly altered in sciatic nerves of HSP^{S139F} mice, specific species of ceramide, SM, and total deoxyceramides are increased in brain tissues of HSP^{S139F} mice.

HSP^{S139F} mice do not exhibit an axonal phenotype, but present with cerebellar demyelination

CMT2F presents with a length-dependent axonal phenotype, having increased severity dependent on the length of the nerve (32), and defects in axonal transport and cytoskeletal elements (33-35). In SH-SY5Y human neuroblastoma cells, $HSPB1^{S135F}$ interfered with anterograde transportation and caused Cdk5-mediated elevations in hyperphosphorylation of neurofilaments (NFs) but did not alter the expression of neurofilament light (NFL) (32). Transgenic mice expressing the human HSP^{S135F} mutation also exhibited hyperphosphorylated NF-heavy (NFH). Therefore, expression and phosphorylation of NFs in HSP^{WT} and HSP^{S139F} mice were examined. Expression of NFL and phosphorylation of NFH remained unaltered in sciatic nerves (Figure S1A & B) and cerebellar tissues of HSP^{S139F} mice (Figure S2A & B).

Transgenic HSP^{S135F} mice, harboring mutant human Hsp27, also exhibited reduced acetylation of α-tubulin in sciatic nerves but retained myelination (36). Therefore, levels of acetylated α-tubulin and myelination in central nervous tissues were assessed. Similar to NF, expression of acetylated α-tubulin nor myelination were altered in sciatic nerves (Figures S1C & D) or cerebellar tissues from either genotype (Figure S2C). Interestingly, HSP^{S139F} mice demonstrated stark cerebellar demyelination (Figure 3). These data suggest that though HSP^{S139F} mice do not exhibit an axonal phenotype at 3 months of age, the S139F mutation in the endogenous Hsp protein may alter myelination in the cerebellum.

HSP^{S139F} impairs muscle strength and motor coordination

CMT2F results in gait abnormalities, as well as atrophy and weakness in distal limbs (37). Therefore, HSP^{WT} and HSP^{S139F} mice were analyzed for locomotor function, grip strength and gait. Gait analysis revealed no significant changes in the HSP^{S139F} mice

compared to the WT (Figure S3). Rotarod performance was assessed to determine motor coordination. Though maximum tolerated speed was similar between genotypes, total run time was significantly decreased in HSP^{S139F} mice (Figure 4A & B). Grip strength was measured with a grip strength meter. All paw grip strength was significantly decreased in HSP^{S139F} mice (Figure 4D). This decrease was primarily due to a significant decrease in forepaw grip strength (Figure 4E &F). These data illustrate distal muscle weakness and motor coordination loss in mice harboring the S139F mutation in *HSPB1*.

DISCUSSION

Point mutations in human *HSPB1* that encode for Hsp27 have been implicated in CMT2F. This study aimed to characterize a novel mouse model containing a point mutation in the endogenous Hsp25 protein in mice, which corresponds to Hsp27 in humans. VLC ceramides and SM species were increased in the brains of HSP^{S139F} mice. These sphingolipids have been implicated in many neurodegenerative diseases and linked to HSP^{S135F} in cells. Alterations in these specific sphingolipids also suggest altered activity of specific ceramide synthases (CerS). In addition, HSP^{S139F} mice exhibited cerebellar demyelination and loss of locomotor coordination. Similar to patients with CMT2F, HSP^{S139F} mice also exhibited decreased muscular strength. Overall, the endogenous S139F mutation in *HSPB1* resulted in similar clinical phenotypes demonstrated in other models of CMT and human patients.

Previous work from our group demonstrated a decrease in ceramides in sciatic nerves, but not brains, of *HSPB1* KO mice as early as one month of age (23). Conversely, in HSP^{S139F} mice ceramides and deoxysphingolipids were not altered in sciatic nerves, while long chain SMs were significantly increased. Examination of cerebellar tissues revealed significantly increased VLC ceramides and SMs. CerS2, which generates VLC ceramides (C22-26), is vital for proper neuronal functioning and is most active in the first several weeks of post-natal mouse development (22, 30). CerS2 deficient mice lack VLC ceramides in the brain and exhibit a progressive loss of myelin stability in trigeminal nerve axons. Contrary to these findings, HSP^{S139F} mice exhibited significantly increased VLC ceramides in cerebellar tissues with a concomitant loss of myelin. These data suggest the potential that levels of VLC sphingolipids, either high or low, may regulate myelin stability. Spassieva et. al. demonstrated that ectopic expression of CerS2 in CerS1 deficient mice reversed Purkinje cell loss and neurodegeneration. This reversal of phenotype was due in part to decreased accumulation of sphingoid bases (38). Purkinje cells were not altered and only sphingosine was elevated in HSP^{S139F}mice. Together these studies suggest that the balance of sphingolipids, specifically VLC sphingolipids, in cerebellar tissues may influence cerebellar pathology.

Accumulation of SM in cerebellar tissues has been implicated in neurodegeneration associated with lysosomal storage disorders. SMs levels are significantly elevated in several visceral organs and the brain in Nieman-Pick Disease (NPD) patients, resulting from mutations or deficiency in acid sphingomyelinase (aSMase). This increased SM resulted in defects in motor coordination and degeneration of cerebellar Purkinje cells (39). Similarly, deficiency or mutations in acid ceramidase result in Farber disease due to the accumulation of ceramide species within the spinal cord and brain (40, 41). These increased ceramides

also lead to Purkinje cell degeneration, as well as impaired motor coordination and balance in mice (42). Though HSP^{S139F} mice did not exhibit loss of Purkinje cells (data not shown), they did exhibit decreased motor coordination as measured by rotarod performance. Taken together, these studies suggest that the increased SMs in HSP^{S139F} mice may contribute to altered motor coordination.

Mutations in the initial enzyme for *de novo* sphingolipid generation, SPT, have been implicated in HSN1 via the accumulation of neurotoxic deoxysphingolipids (14). Treatment with exogenous deoxysphinganine, the precursor for deoxyceramides, resulted in mitochondrial disfunction in motor and sensory neurons (43). Similarly, deoxysphinganine treatment decreased neurite formation in cultured sensory neurons and altered neurofilament structure (14). Patients with HSN1C exhibited slowed conduction velocity in motor nerves of the arms and legs, suggesting damage to both myelin and axons in peripheral nerves. This was accompanied by increased deoxysphinganine, deoxysphingosine and deoxyceramides (44). Deoxyceramide, but not deoxysphinganine, was elevated in brain tissues of HSP^{S139F} mice, suggesting that these sphingolipid species may contribute to demyelination, loss of motor control, and decreased strength.

Disruption in myelin homeostasis is typically associated with CMT1; however, recent work by Hwang et. al. also demonstrated patients with mutations in *NEFL* exhibited decreased volume of white matter, suggesting the possibility of myelin defects in patients with mutations associated with both CMT1 and CMT2 phenotypes (45). Our data documented significant cerebellar demyelination in HSP^{S135F} mice, which we hypothesized would model CMT2F. Interestingly loss of CerS2, which generates VLC ceramides, has been implicated in the disruption of myelination in the brain, including the cerebellum (46). Additionally, patients with NPD accumulate SM and exhibit impaired myelination in the brain (47). Conversely, inhibition or genetic deletion of neutral sphingomyelinase 2 in oligodendrocytes reduced ceramide levels and promoted remyelination in a mouse model (48). Further, mice harboring CerS2 deletion specifically in oligodendrocytes demonstrated reduced myelination in peripheral and central nervous systems, impaired motor coordination, and weakness in paw strength (49). Despite the major role oligodendrocytes play in proper myelination of neurons, there is a gap in knowledge as to the role of sphingolipid metabolism in these cells in the context of CMT2F. While these studies suggest that dysregulation of sphingolipids may alter myelin homeostasis, it is also possible that the HSP^{S135F} mouse may not accurately model CMT2F. Mutations in *HSPB1* are also associated with amyotrophic lateral sclerosis (ALS) which can present with axonal loss and demyelination (50, 51). Mutations in connexon proteins in oligodendrocytes lead to myelination defects and are more commonly associated with CMT1X, a subset which interestingly displays both demyelinating and axonal phenotypes (52, 53). Additional investigation into motor nerve conduction velocity (MNCV) and compound muscle action potential (CMAP) could further validate the HSP^{S139F} mouse as a novel model for CMT and/or HSN.

Phosphorylated neurofilament and acetylated tubulin have been described as molecular pathological markers for mutant *HSPB1* mediated axonopathy. Neurofilaments are an important molecule in axons responsible for radial growth and phosphorylation of these molecules have been established to be a determinant of axon fiber caliber, plasticity and

stability (54). Previous models for CMT have demonstrated alterations in neurofilament in spinal cords and sciatic nerves. Cultured motor neurons, derived from E13 mouse spinal cord, transfected with HSBP1^{S135F} showed disruption in NF networks and aggregation of NFL (33). Sciatic nerves from transgenic HSP^{S135F} mice also exhibited increased phosphorylated NFH at 10 months of age (29). SH-SY5Y neuroblastomas expressing the human HSP^{S135F} mutation demonstrated hyperphosphorylated NFs; however, expression remained unaltered. Acetylated α-tubulin is a cytoskeletal component in neurons that regulate transport along microtubules (55), and has also been described as molecular markers for mutant *HSPB1* mediated axonopathy (36). Transgenic HSP^{S135F} mice exhibited a significant decrease in acetylated α-tubulin within sciatic nerves (29, 36). However, transfected HSP^{S135F} HT-22 cells displayed unaltered acetylated α-tubulin (23). Mice harboring the S139F mutation in the endogenous Hsp25 protein, did not exhibit altered NF expression or phosphorylation, nor altered expression of acetylated α-tubulin, in sciatic nerves or cerebellar tissues at 3 months of age. Interestingly, at this time point motor coordination and grip strength were already decreased. It is possible that the S139F mutation in the endogenous protein did not significantly alter NF or acetylated α-tubulin at 3 months of age, but that this may develop with increasing age, as patients with CMT exhibit highly variable progression of disease, with early onset ranging from 21 to 67 years of age (32).

CMT presents clinically with abnormal gait, loss of distal sensation and reflexes. Recent studies investigating common mutations in CMT2 in *C. elegans* demonstrated that mutations in Hsp25 did not alter locomotion, but significantly altered muscle morphology (56). In mice expressing the S135F mutant form of Hsp27, locomotor coordination and all paw grip strength decreased after 5 months of age (29). In the present study HSP^{S139F} mice demonstrated phenotypic changes at 3 months of age. Muscular strength and locomotor coordination were both decreased in the HSP^{S139F} mice, providing potential insight into the effects of the S139F mutation on clinical phenotypes associated with CMT2F. These data indicate loss of both coordination and muscle strength in HSP^{S139F} mice, demonstrating similar phenotypes to other models of CMT, as well as clinical presentations of CMT.

The S139F endogenous mutation of *HSPB1* in mice, rather than the overexpression of the human mutation or knockout of *HSPB1*, may prove to be a viable model for CMT. HSP^{S135F} mice displayed CMT2F-like loss of motor control and reduction in distal strength. Sphingolipid metabolism panels and histological investigation determined that HSP^{S135F} mice do not exhibit sciatic nerve pathology but do exhibit cerebellar pathology, potentially due to CerS2 activity. Utilization of novel mouse models will allow for investigations into the mechanisms by which these mutations result in disease and may identify novel therapeutic targets. Based on our studies implicating altered sphingolipid metabolism, cerebral demyelination, and decreased muscle strength and locomotor coordination, HSP^{S139F} mice may serve as an appropriate model for CMT2F or other HSANs.

Supplementary Material

Refer to Web version on PubMed Central for supplementary material.

ACKNOWLEDGEMENTS

Lipidomic analyses in this publication were provided by Stony Brook University Biological Mass Spectrometry Shared Resource Core supported the National Cancer Institute at the National Institutes of Health P01 CA097132, and the University of Arizona Cancer Center Analytical Chemistry Shared Resource Core supported by the National Cancer Institute at the National Institutes of Health P30 CA023074. Histology samples included in this publication/press release were provided by the University of Arizona Cancer Center Tissue Acquisition and Cellular/Molecular Analysis Shared Resource (TACMASR) supported by the National Cancer Institute at the National Institutes of Health P30 CA023074.

Grant support

This work was supported by the National Institute for Neurologic Disorders and Stroke at the National Institutes of Health R03 NS111420 (AJS).

ABBREVIATIONS

CMT	Charcot-Marie-Tooth
HSPB1	heat-shock protein B1
Hsp27	heat shock protein 27
dHMSNB2	distal hereditary motor and sensory neuropathy type 2B
SM	sphingomyelin
SPT	serine palmitoyl transferase
HSAN	hereditary sensory and autonomic neuropathy
CerS	ceramide synthases
VLC	very-long chain
NF	neurofilament
NFL	neurofilament light
NFH	neurofilament heavy
NPD	Nieman-Pick Disease
aSMase	acid sphingomyelinase
CMAP	compound muscle action potential
MNCV	motor nerve conduction velocity

References

1. Timmerman V, Strickland AV, and Zuchner S (2014) Genetics of Charcot-Marie-Tooth (CMT) Disease within the Frame of the Human Genome Project Success. Genes (Basel) 5, 13–32 [PubMed: 24705285]
2. England JD, Gronseth GS, Franklin G, Carter GT, Kinsella LJ, Cohen JA, Asbury AK, Szigeti K, Lupski JR, Latov N, Lewis RA, Low PA, Fisher MA, Herrmann DN, Howard JF Jr., Lauria G, Miller RG, Polydefkis M, Sumner AJ, and American Academy of, N. (2009) Practice Parameter:

evaluation of distal symmetric polyneuropathy: role of autonomic testing, nerve biopsy, and skin biopsy (an evidence-based review). Report of the American Academy of Neurology, American Association of Neuromuscular and Electrodiagnostic Medicine, and American Academy of Physical Medicine and Rehabilitation. Neurology 72, 177–184 [PubMed: 19056667]

3. England JD, Gronseth GS, Franklin G, Carter GT, Kinsella LJ, Cohen JA, Asbury AK, Szigeti K, Lupski JR, Latov N, Lewis RA, Low PA, Fisher MA, Herrmann DN, Howard JF Jr., Lauria G, Miller RG, Polydefkis M, Sumner AJ, and American Academy of, N. (2009) Practice Parameter: evaluation of distal symmetric polyneuropathy: role of laboratory and genetic testing (an evidence-based review). Report of the American Academy of Neurology, American Association of Neuromuscular and Electrodiagnostic Medicine, and American Academy of Physical Medicine and Rehabilitation. Neurology 72, 185–192 [PubMed: 19056666]
4. Harding AE, and Thomas PK (1980) The clinical features of hereditary motor and sensory neuropathy types I and II. Brain 103, 259–280 [PubMed: 7397478]
5. Harding AE, and Thomas PK (1980) Genetic aspects of hereditary motor and sensory neuropathy (types I and II). J Med Genet 17, 329–336 [PubMed: 7218272]
6. Thomas PK, and Harding AE (1993) Inherited neuropathies: the interface between molecular genetics and pathology. Brain Pathol 3, 129–133 [PubMed: 8293174]
7. Dyck PJ, and Lambert EH (1968) Lower motor and primary sensory neuron diseases with peroneal muscular atrophy. I. Neurologic, genetic, and electrophysiologic findings in hereditary polyneuropathies. Arch Neurol 18, 603–618 [PubMed: 4297451]
8. Harel T, and Lupski JR (2014) Charcot-Marie-Tooth disease and pathways to molecular based therapies. Clin Genet 86, 422–431 [PubMed: 24697164]
9. Evgrafov OV, Mersiyanova I, Irobi J, Van Den Bosch L, Dierick I, Leung CL, Schagina O, Verpoorten N, Van Impe K, Fedotov V, Dadali E, Auer-Grumbach M, Windpassinger C, Wagner K, Mitrovic Z, Hilton-Jones D, Talbot K, Martin JJ, Vasserman N, Tverskaya S, Polyakov A, Liem RK, Gettemans J, Robberecht W, De Jonghe P, and Timmerman V (2004) Mutant small heat-shock protein 27 causes axonal Charcot-Marie-Tooth disease and distal hereditary motor neuropathy. Nat Genet 36, 602–606 [PubMed: 15122254]
10. Haslbeck M, Franzmann T, Weinfurtner D, and Buchner J (2005) Some like it hot: the structure and function of small heat-shock proteins. Nat Struct Mol Biol 12, 842–846 [PubMed: 16205709]
11. Hsu AL, Murphy CT, and Kenyon C (2003) Regulation of aging and age-related disease by DAF-16 and heat-shock factor. Science 300, 1142–1145 [PubMed: 12750521]
12. Latchman DS (2002) Protection of neuronal and cardiac cells by HSP27. Prog Mol Subcell Biol 28, 253–265 [PubMed: 11908064]
13. Schwartz NU (2019) Charcot-Marie-Tooth 2F (Hsp27 mutations): A review. Neurobiol Dis 130, 104505 [PubMed: 31212070]
14. Penno A, Reilly MM, Houlden H, Laura M, Rentsch K, Niederkofler V, Stoeckli ET, Nicholson G, Eichler F, Brown RH Jr., von Eckardstein A, and Hornemann T (2010) Hereditary sensory neuropathy type 1 is caused by the accumulation of two neurotoxic sphingolipids. J Biol Chem 285, 11178–11187 [PubMed: 20097765]
15. Hannun YA, and Obeid LM (2011) Many ceramides. J Biol Chem 286, 27855–27862 [PubMed: 21693702]
16. Mullen TD, Hannun YA, and Obeid LM (2012) Ceramide synthases at the centre of sphingolipid metabolism and biology. The Biochemical journal 441, 789–802 [PubMed: 22248339]
17. Venkataraman K, Riebeling C, Bodennec J, Riezman H, Allegood JC, Sullards MC, Merrill AH Jr., and Futerman AH (2002) Upstream of growth and differentiation factor 1 (uog1), a mammalian homolog of the yeast longevity assurance gene 1 (LAG1), regulates N-stearoyl-sphinganine (C18-(dihydro)ceramide) synthesis in a fumonisin B1-independent manner in mammalian cells. J Biol Chem 277, 35642–35649 [PubMed: 12105227]
18. Sentelle RD, Senkal CE, Jiang W, Ponnusamy S, Gencer S, Selvam SP, Ramshesh VK, Peterson YK, Lemasters JJ, Szulc ZM, Bielawski J, and Ogretmen B (2012) Ceramide targets autophagosomes to mitochondria and induces lethal mitophagy. Nat Chem Biol 8, 831–838 [PubMed: 22922758]

19. Jiang JC, Kirchman PA, Zagulski M, Hunt J, and Jazwinski SM (1998) Homologs of the yeast longevity gene LAG1 in Caenorhabditis elegans and human. Genome Res 8, 1259–1272 [PubMed: 9872981]
20. Levy M, and Futerman AH (2010) Mammalian ceramide synthases. IUBMB Life 62, 347–356 [PubMed: 20222015]
21. Zhao L, Spassieva SD, Jucius TJ, Shultz LD, Shick HE, Macklin WB, Hannun YA, Obeid LM, and Ackerman SL (2011) A deficiency of ceramide biosynthesis causes cerebellar purkinje cell neurodegeneration and lipofuscin accumulation. PLoS genetics 7, e1002063 [PubMed: 21625621]
22. Imgrund S, Hartmann D, Farwanah H, Eckhardt M, Sandhoff R, Degen J, Gieselmann V, Sandhoff K, and Willecke K (2009) Adult ceramide synthase 2 (CERS2)-deficient mice exhibit myelin sheath defects, cerebellar degeneration, and hepatocarcinomas. J Biol Chem 284, 33549–33560 [PubMed: 19801672]
23. Schwartz NU, Linzer RW, Truman JP, Gurevich M, Hannun YA, Senkal CE, and Obeid LM (2018) Decreased ceramide underlies mitochondrial dysfunction in Charcot-Marie-Tooth 2F. FASEB J 32, 1716–1728 [PubMed: 29133339]
24. Choi S, Snider JM, Olakkengil N, Lambert JM, Anderson AK, Ross-Evans JS, Cowart LA, and Snider AJ (2018) Myristate-induced endoplasmic reticulum stress requires ceramide synthases 5/6 and generation of C14-ceramide in intestinal epithelial cells. FASEB J 32, 5724–5736 [PubMed: 29768040]
25. Schwartz NU, Mileva I, Gurevich M, Snider J, Hannun YA, and Obeid LM (2019) Quantifying 1-deoxydihydroceramides and 1-deoxyceramides in mouse nervous system tissue. Prostaglandins Other Lipid Mediat 141, 40–48 [PubMed: 30790665]
26. Bielawski J, Pierce JS, Snider J, Rembiesa B, Szulc ZM, and Bielawska A (2010) Sphingolipid analysis by high performance liquid chromatography-tandem mass spectrometry (HPLC-MS/MS). Adv Exp Med Biol 688, 46–59 [PubMed: 20919645]
27. Bligh EG, and Dyer WJ (1959) A RAPID METHOD OF TOTAL LIPID EXTRACTION AND PURIFICATION. Canadian Journal of Biochemistry and Physiology 37, 911–917 [PubMed: 13671378]
28. Van Veldhoven PP, and Bell RM (1988) Effect of harvesting methods, growth conditions and growth phase on diacylglycerol levels in cultured human adherent cells. Biochimica et Biophysica Acta (BBA) - Lipids and Lipid Metabolism 959, 185–196 [PubMed: 3349097]
29. Lee J, Jung SC, Joo J, Choi YR, Moon HW, Kwak G, Yeo HK, Lee JS, Ahn HJ, Jung N, Hwang S, Rheey J, Woo SY, Kim JY, Hong YB, and Choi BO (2015) Overexpression of mutant HSP27 causes axonal neuropathy in mice. J Biomed Sci 22, 43 [PubMed: 26141737]
30. Ben-David O, Pewzner-Jung Y, Brenner O, Laviad EL, Kogot-Levin A, Weissberg I, Biton IE, Pienik R, Wang E, Kelly S, Alroy J, Raas-Rothschild A, Friedman A, Brugger B, Merrill AH Jr., and Futerman AH (2011) Encephalopathy caused by ablation of very long acyl chain ceramide synthesis may be largely due to reduced galactosylceramide levels. J Biol Chem 286, 30022–30033 [PubMed: 21705317]
31. Ginkel C, Hartmann D, vom Dorp K, Zlomuzica A, Farwanah H, Eckhardt M, Sandhoff R, Degen J, Rabionet M, Dere E, Dormann P, Sandhoff K, and Willecke K (2012) Ablation of neuronal ceramide synthase 1 in mice decreases ganglioside levels and expression of myelin-associated glycoprotein in oligodendrocytes. J Biol Chem 287, 41888–41902 [PubMed: 23074226]
32. Greenbaum L, Ben-David M, Nikitin V, Gera O, Barel O, Hersalis-Eldar A, Shamash J, Shimshoviz N, Reznik-Wolf H, Shohat M, Dominissini D, Pras E, and Dori A (2021) Early and late manifestations of neuropathy due to HSPB1 mutation in the Jewish Iranian population. Ann Clin Transl Neurol 8, 1260–1268 [PubMed: 33973728]
33. Zhai J, Lin H, Julien JP, and Schlaepfer WW (2007) Disruption of neurofilament network with aggregation of light neurofilament protein: a common pathway leading to motor neuron degeneration due to Charcot-Marie-Tooth disease-linked mutations in NFL and HSPB1. Hum Mol Genet 16, 3103–3116 [PubMed: 17881652]
34. Holmgren A, Bouhy D, De Winter V, Asselbergh B, Timmermans JP, Irobi J, and Timmerman V (2013) Charcot-Marie-Tooth causing HSPB1 mutations increase Cdk5-mediated phosphorylation of neurofilaments. Acta Neuropathol 126, 93–108 [PubMed: 23728742]

35. Almeida-Souza L, Asselbergh B, d'Ydewalle C, Moonens K, Goethals S, de Winter V, Azmi A, Irobi J, Timmermans JP, Gevaert K, Remaut H, Van Den Bosch L, Timmerman V, and Janssens S (2011) Small heat-shock protein HSPB1 mutants stabilize microtubules in Charcot-Marie-Tooth neuropathy. J Neurosci 31, 15320–15328 [PubMed: 22031878]
36. d'Ydewalle C, Krishnan J, Chiheb DM, Van Damme P, Irobi J, Kozikowski AP, Vanden Berghe P, Timmerman V, Robberecht W, and Van Den Bosch L (2011) HDAC6 inhibitors reverse axonal loss in a mouse model of mutant HSPB1-induced Charcot-Marie-Tooth disease. Nat Med 17, 968–974 [PubMed: 21785432]
37. Bienfait HM, Baas F, Koelman JH, de Haan RJ, van Engelen BG, Gabreels-Festen AA, Ongerboer de Visser BW, Meggouh F, Weterman MA, De Jonghe P, Timmerman V, and de Visser M (2007) Phenotype of Charcot-Marie-Tooth disease Type 2. Neurology 68, 1658–1667 [PubMed: 17502546]
38. Spassieva SD, Ji X, Liu Y, Gable K, Bielawski J, Dunn TM, Bieberich E, and Zhao L (2016) Ectopic expression of ceramide synthase 2 in neurons suppresses neurodegeneration induced by ceramide synthase 1 deficiency. Proc Natl Acad Sci U S A 113, 5928–5933 [PubMed: 27162368]
39. Otterbach B, and Stoffel W (1995) Acid sphingomyelinase-deficient mice mimic the neurovisceral form of human lysosomal storage disease (Niemann-Pick disease). Cell 81, 1053–1061 [PubMed: 7600574]
40. Koch J, Gartner S, Li CM, Quintern LE, Bernardo K, Levran O, Schnabel D, Desnick RJ, Schuchman EH, and Sandhoff K (1996) Molecular cloning and characterization of a full-length complementary DNA encoding human acid ceramidase. Identification Of the first molecular lesion causing Farber disease. J Biol Chem 271, 33110–33115 [PubMed: 8955159]
41. Jameson RA, Holt PJ, and Keen JH (1987) Farber's disease (lysosomal acid ceramidase deficiency). Ann Rheum Dis 46, 559–561 [PubMed: 3662645]
42. Wang K, Xu R, Schrandt J, Shah P, Gong YZ, Preston C, Wang L, Yi JK, Lin CL, Sun W, Spyropoulos DD, Rhee S, Li M, Zhou J, Ge S, Zhang G, Snider AJ, Hannun YA, Obeid LM, and Mao C (2015) Alkaline Ceramidase 3 Deficiency Results in Purkinje Cell Degeneration and Cerebellar Ataxia Due to Dyshomeostasis of Sphingolipids in the Brain. PLoS Genet 11, e1005591 [PubMed: 26474409]
43. Wilson ER, Kugathasan U, Abramov AY, Clark AJ, Bennett DLH, Reilly MM, Greensmith L, and Kalmar B (2018) Hereditary sensory neuropathy type 1-associated deoxysphingolipids cause neurotoxicity, acute calcium handling abnormalities and mitochondrial dysfunction in vitro. Neurobiol Dis 117, 1–14 [PubMed: 29778900]
44. Saba S, Chen Y, Maddipati KR, Hackett M, Hu B, and Li J (2020) Demyelination in hereditary sensory neuropathy type-1C. Ann Clin Transl Neurol 7, 1502–1512 [PubMed: 32730653]
45. Hwang S, Park CH, Kim RE, Kim HJ, Choi YS, Kim SA, Yoo JH, Chung KW, Choi BO, and Lee HW (2021) Cerebellar White Matter Abnormalities in Charcot-Marie-Tooth Disease: A Combined Volumetry and Diffusion Tensor Imaging Analysis. J Clin Med 10
46. Maitre M, Jeltsch-David H, Okechukwu NG, Klein C, Patte-Mensah C, and Mensah-Nyagan AG (2023) Myelin in Alzheimer's disease: culprit or bystander? Acta Neuropathol Commun 11, 56 [PubMed: 37004127]
47. Bernardo A, De Nuccio C, Visentin S, Martire A, Minghetti L, Popoli P, and Ferrante A (2021) Myelin Defects in Niemann-Pick Type C Disease: Mechanisms and Possible Therapeutic Perspectives. Int J Mol Sci 22
48. Yoo SW, Agarwal A, Smith MD, Khuder SS, Baxi EG, Thomas AG, Rojas C, Moniruzzaman M, Slusher BS, Bergles DE, Calabresi PA, and Haughey NJ (2020) Inhibition of neutral sphingomyelinase 2 promotes remyelination. Sci Adv 6
49. Teo JD, Marian OC, Spiteri AG, Nicholson M, Song H, Khor JXY, McEwen HP, Ge A, Sen MK, Piccio L, Fletcher JL, King NJC, Murray SS, Bruning JC, and Don AS (2023) Early microglial response, myelin deterioration and lethality in mice deficient for very long chain ceramide synthesis in oligodendrocytes. Glia 71, 1120–1141 [PubMed: 36583573]
50. Katz M, Davis M, Garton FC, Henderson R, Bharti V, Wray N, and McCombe P (2020) Mutations in heat shock protein beta-1 (HSPB1) are associated with a range of clinical phenotypes related to different patterns of motor neuron dysfunction: A case series. J Neurol Sci 413, 116809 [PubMed: 32334137]

51. Heilman PL, Song S, Miranda CJ, Meyer K, Srivastava AK, Knapp A, Wier CG, Kaspar BK, and Kolb SJ (2017) HSPB1 mutations causing hereditary neuropathy in humans disrupt non-cell autonomous protection of motor neurons. Exp Neurol 297, 101–109 [PubMed: 28797631]
52. Olympiou M, Sargiannidou I, Markoullis K, Karaiskos C, Kagiava A, Kyriakoudi S, Abrams CK, and Kleopa KA (2016) Systemic inflammation disrupts oligodendrocyte gap junctions and induces ER stress in a model of CNS manifestations of X-linked Charcot-Marie-Tooth disease. Acta Neuropathol Commun 4, 95 [PubMed: 27585976]
53. Sargiannidou I, Vavlitou N, Aristodemou S, Hadjisavvas A, Kyriacou K, Scherer SS, and Kleopa KA (2009) Connexin32 mutations cause loss of function in Schwann cells and oligodendrocytes leading to PNS and CNS myelination defects. J Neurosci 29, 4736–4749 [PubMed: 19369543]
54. Pant HC, and Veeranna. (1995) Neurofilament phosphorylation. Biochem Cell Biol 73, 575–592 [PubMed: 8714676]
55. Nekooki-Machida Y, and Hagiwara H (2020) Role of tubulin acetylation in cellular functions and diseases. Med Mol Morphol 53, 191–197 [PubMed: 32632910]
56. Soh MS, Cheng X, Vijayaraghavan T, Vernon A, Liu J, and Neumann B (2020) Disruption of genes associated with Charcot-Marie-Tooth type 2 lead to common behavioural, cellular and molecular defects in Caenorhabditis elegans. PloS one 15, e0231600 [PubMed: 32294113]
57. Low BE, Kutny PM, Wiles MV, Simple, Efficient CRISPR-Cas9-Mediated Gene Editing in Mice: Strategies and Methods, Methods Mol Biol 1438 (2016) 19–53, 10.1007/978-1-4939-3661-8_2. [PubMed: 27150082]
58. Oliveros JC, Franch M, Tabas-Madrid D, San-León D, Montoliu L, Cubas P, Pazos F, Breaking-Cas-interactive design of guide RNAs for CRISPR-Cas experiments for ENSEMBL genomes, Nucleic Acids Res 44 (W1) (2016) W267–W271, 10.1093/nar/gkw407. Epub 2016 May 10. [PubMed: 27166368]
59. Richardson CD, Ray GJ, DeWitt MA, Curie GL, Corn JE, Enhancing homology-directed genome editing by catalytically active and inactive CRISPRCas9 using asymmetric donor DNA, Nat Biotechnol 34 (3) (2016) 339–344, 10.1038/nbt.3481. Epub 2016 Jan 20. [PubMed: 26789497]
60. Fu Y, Sander JD, Reyon D, Cascio VM, Joung JK, Improving CRISPR-Cas nuclease specificity using truncated guide RNAs, Nat Biotechnol 32 (3) (2014) 279–284, 10.1038/nbt.2808. Epub 2014 Jan 26. [PubMed: 24463574]

Highlights

- Novel murine *HSPB1* mutations model human manifestations of CMT.
- Sphingolipid profiles are altered in the brain of *HSPB1* mutant mice.
- Novel murine *HSPB1* mutation results in cerebellar demyelination.

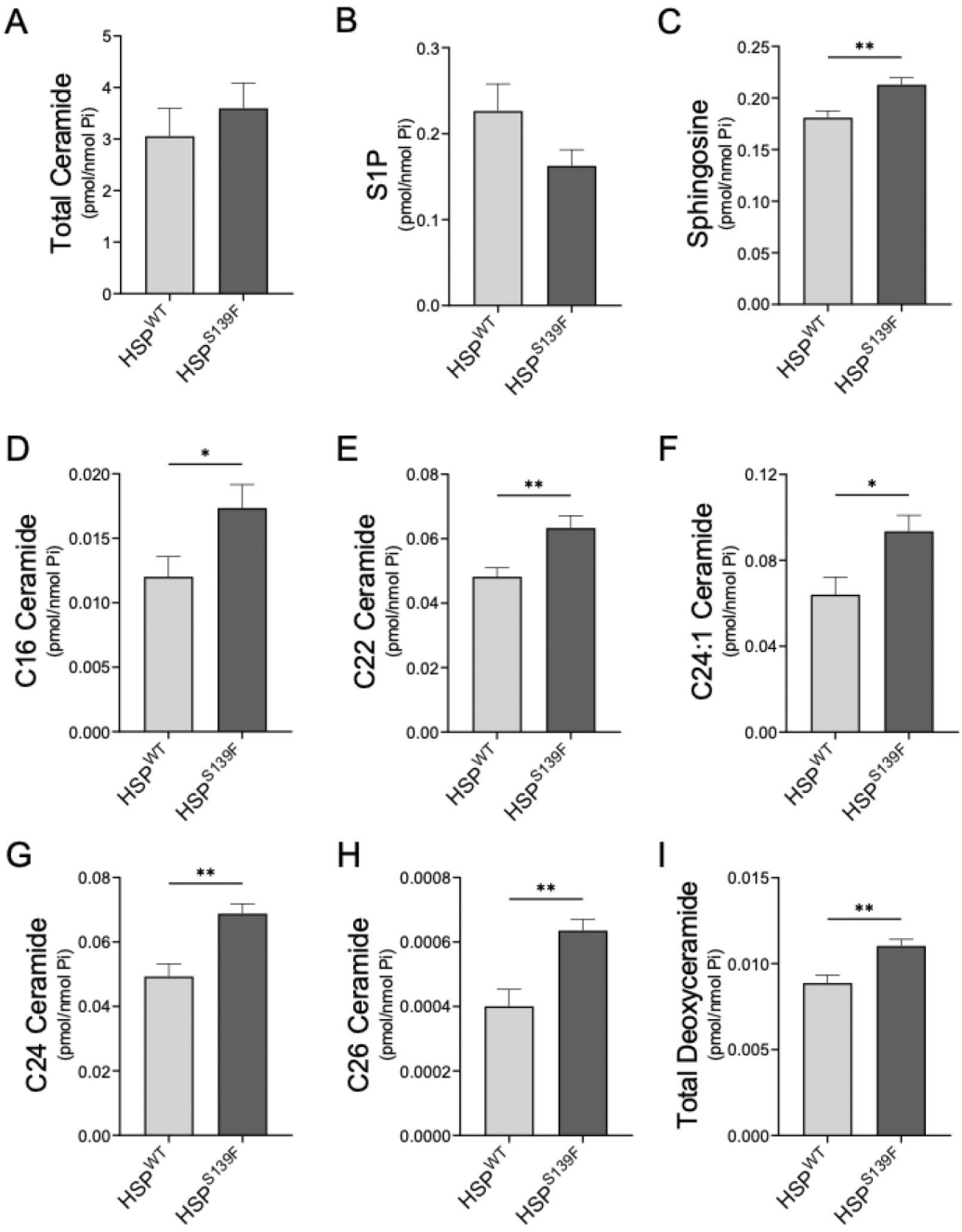

Figure 1. Ceramides and deoxyceramides are altered in brain tissues HSP^{S139F} mice.

Cerebellar samples were analyzed from HSP^{WT} and HSP^{S139F} mice at 3-months of age for A) total ceramide, B) S1P, C) sphingosine, D-) individual ceramide species, as well as I) deoxyceramides using LC-MS/MS and normalized to total lipid phosphate (Pi). Data represent mean ± SEM, n=8 mice. *p<0.05, **p<0.01.

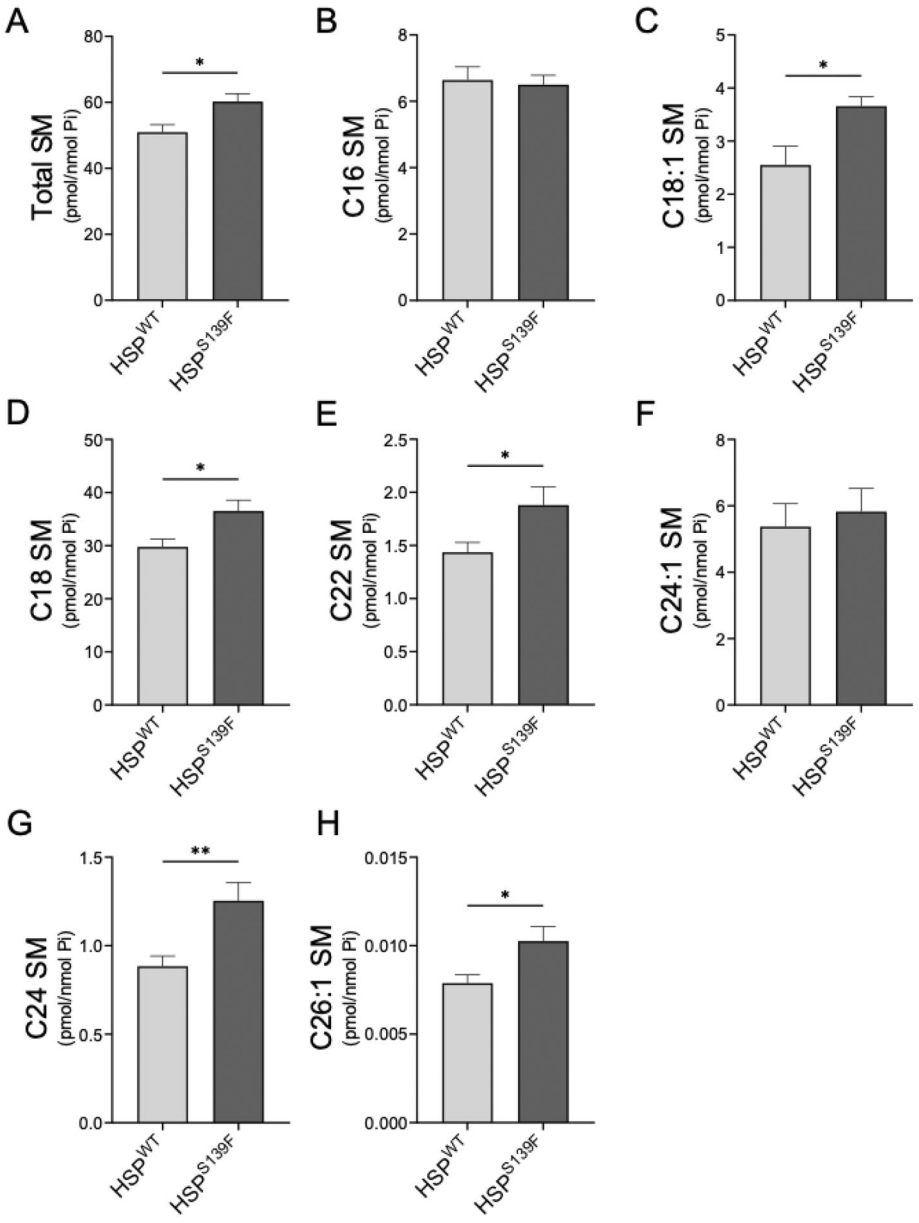

Figure 2. Sphingomyelins are altered in brain tissues HSP^{S139F} mice.

Cerebellar samples were analyzed from HSP^{WT} and HSP^{S139F} mice at 3-months of age for A) total SM, and B-H) individual SM species by LC-MS/MS and normalized to total lipid phosphate (Pi). Data represent mean ± SEM, n=8 mice. *p<0.05, **p<0.01.

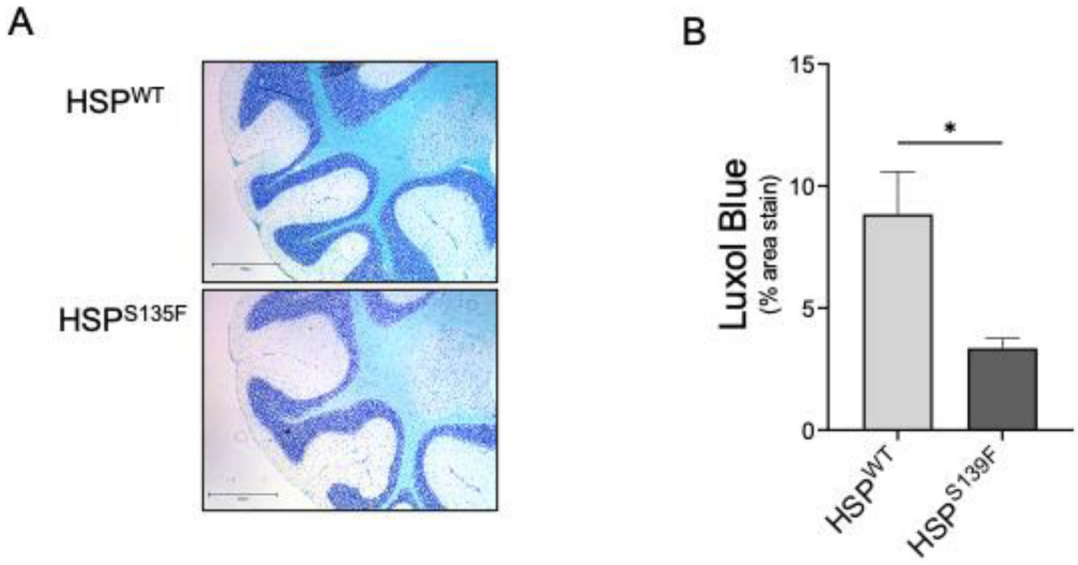

Figure 3. HSP^{S139F} mice demonstrate cerebellar demyelination.

Brains of 3-month-old HSP^{WT} and HSP^{S139F} mice were collected and stained for myelination using Luxol fast blue. A) Representative images of cerebellum and B) quantification of Luxol staining using ImageJ. E-H). Magnification 4x, scale bar = 600μm. Data represent mean ± SEM, n≥7. *p<0.05.

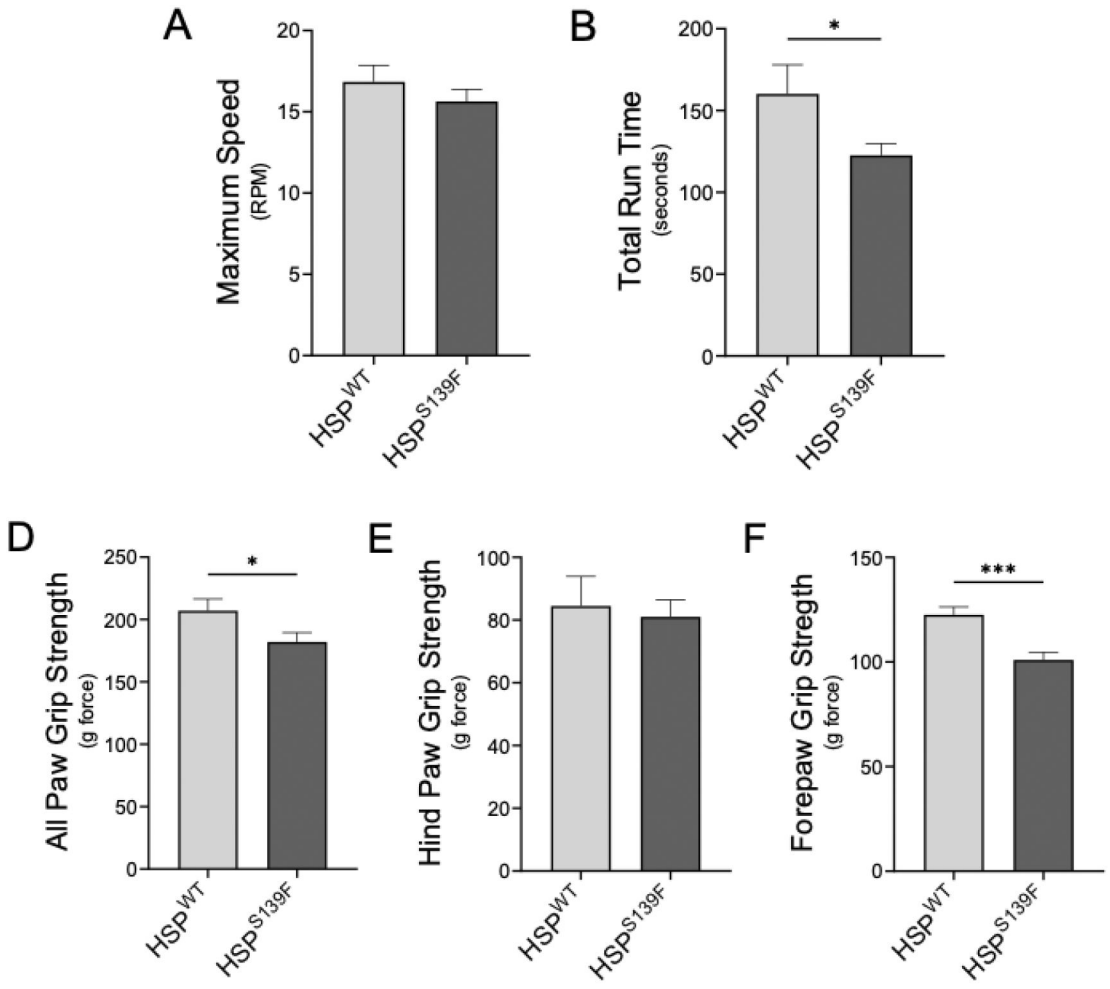

Figure 4. Motor coordination and grip strength are reduced in HSP^{S139F} mice.

Coordination of mice was tested using a Rotarod Rotamex-5 at 3-months of age. A) Maximum tolerated speed and B) total run time and were assessed. Muscular strength in the D) all paws, E) hind paws and F) forepaws of HSP^{WT} and HSP^{S139F} mice was assessed at 3-months of age using a grip-strength meter. Data represent the mean ± SEM for 5 separate tests; n=8 mice; *p< 0.05, ***p < 0.0001.

Table 1:

Sequence alignment of human and mouse *HSPB1* gene.

Human	VVEITGKHEERQDEHGYI**S**RCFTR 135
HSP^{WT} Mouse	VVEITGKHEERQDEHGYI**S**RCFTR 139
HSP^{S139F} Mouse	VVEITGKHEERQDEHGYI**F**RCFTR 139